

SPViT: Enabling Faster Vision Transformers via Soft Token Pruning

Zhenglun Kong^{1*} Peiyan Dong^{1*} Xiaolong Ma¹ Xin Meng³ Wei Niu²
Mengshu Sun¹ Bin Ren² Minghai Qin⁴ Hao Tang⁴ Yanzhi Wang^{1,5}

¹Northeastern University ²College of William and Mary ³Peking University ⁴CVL, ETH Zurich ⁵CoCoPIE LLC

{kong.zhe, dong.pe, ma.xiaol, sun.meng, yanzhi.wang}@northeastern.edu, wniu@email.wm.edu, bren@cs.wm.edu, 1601214372@pku.edu.cn, minghai.qin@jacobs.ucsd.edu, hao.tang@vision.ee.ethz.ch

Abstract

Recently, Vision Transformer (ViT) has continuously established new milestones in the computer vision field, while the high computation and memory cost makes its propagation in industrial production difficult. Pruning, a traditional model compression paradigm for hardware efficiency, has been widely applied in various DNN structures. Nevertheless, it stays ambiguous on how to perform exclusive pruning on the ViT structure. Considering three key points: the structural characteristics, the internal data pattern of ViTs, and the related edge device deployment, we leverage the input token sparsity and propose a computation-aware soft pruning framework, which can be set up on vanilla Transformers of both flatten and CNN-type structures, such as Pooling-based ViT (PiT). More concretely, we design a dynamic attention-based multi-head token selector, which is a lightweight module for adaptive instance-wise token selection. We further introduce a soft pruning technique, which integrates the less informative tokens generated by the selector module into a package token that will participate in subsequent calculations rather than being completely discarded. Our framework is bound to the trade-off between accuracy and computation constraints of specific edge devices through our proposed computation-aware training strategy. Experimental results show that our framework significantly reduces the computation cost of ViTs while maintaining comparable performance on image classification. Moreover, our framework can guarantee the identified model to meet resource specifications of mobile devices and FPGA, and even achieve the real-time execution of DeiT-T on mobile platforms. For example, our method reduces the latency of DeiT-T to 26 ms (26%~41% superior to existing works) on the mobile device with 0.25%~4% higher top-1 accuracy on ImageNet. Our code will be released soon.

*Both authors contributed equally.

1. Introduction

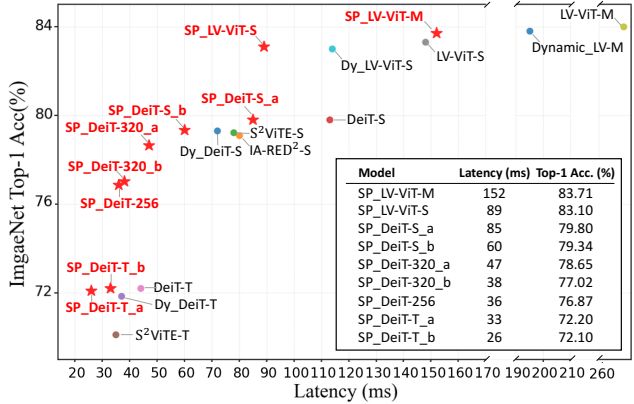


Figure 1. Comparison of different pruning methods with various accuracy-latency trade-offs. We can increase the accuracy of light weight models at similar latency, and expedite larger models with negligible decrease of accuracy. Models are tested on Samsung Galaxy S20.

Recently, a new trend of leveraging Transformer architecture [61] into the computer vision domain has emerged [12, 19, 28, 33, 36, 57, 71, 83]. The Vision Transformer (ViT), which solely exploits the self-attention mechanism that inherits from the Transformer architecture, has set up many state-of-the-art (SOTA) records in image classifications [6, 21, 60], object detection [1, 3, 17, 47], tracking [14, 46, 72], semantic segmentation [15, 20, 84], depth estimation [40, 75], human pose estimation [39], 3D object animation [7], image retrieval [22], and image enhancement [8, 44, 74]. However, despite the impressive general results, ViTs have sacrificed lightweight model capacity, portability, and trainability in return for high accuracy. The mass amount of computations brought by operations (e.g. Conv, MatMul, Add) in existing models remains a setback for edge device deployment.

Pruning, as one of the most straightforward and effective methods to reduce network dimensions, is thoroughly

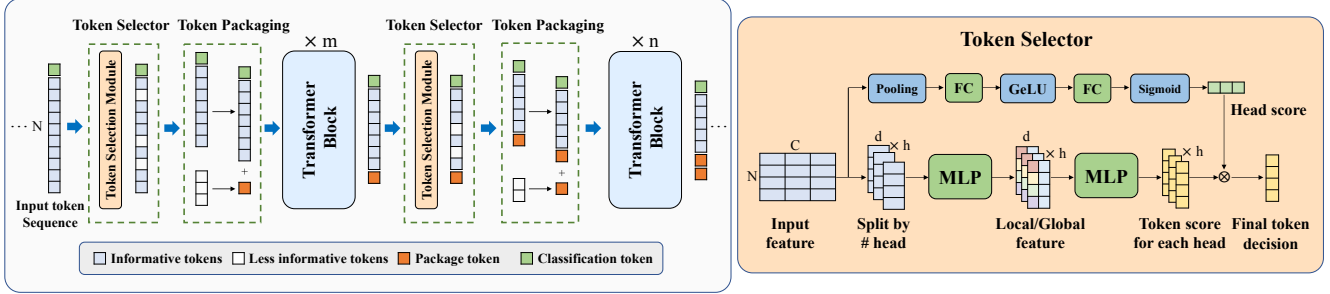


Figure 2. Overall workflow. Left figure: Token selector is inserted multiple times throughout the model, along with the token packaging technique to generate a package token from the less informative tokens. The package token is concatenated with the informative tokens to be fed in the following transformer blocks. Right figure: Our attention-based multi-head token selector to obtain token scores for keep/prune decisions.

explored in convolution-based neural networks [30, 42, 54], yet its application in self-attention-based neural networks remain scarce [27, 38, 56, 62]. Currently, some pioneering works are exploring ViT pruning. However, there still exists a gap between the actual device deployment and acceleration in their frameworks. For instance, attention head pruning [11] performs weight pruning on the transformation matrix (W_Q , W_K , W_V) before the multi-head self-attention (MSA) operation. It is an inefficient way for computation reduction because only part of the ViT computations (i.e., MSA) can be alleviated (see Sec. 3 for justification). In a lightweight model, head pruning cannot guarantee an ideal pruning rate without significant accuracy deterioration. Static token pruning [53] reduces the number of input tokens by a fixed ratio for different images, which restricts the image pruning rate, ignoring the fact that the high-level information of each image varies both in the region size and location. Furthermore, it is difficult for the deployment on edge devices since newly introduced operations (e.g., Argsort) are currently not well supported by many frameworks [50]. In contrast, dynamic token pruning [48] deletes redundant tokens based on the inherent image characteristics to achieve a per-image adaptive pruning rate. However, this method implies a potentially huge search space, which will easily cause a limited overall pruning rate or undermined accuracy if the token selection mechanism is not carefully designed. In addition, the pruning mechanism in [48] unreservedly discards less informative tokens, which results in the loss of the informative part of the removed tokens.

In this paper, we manage to overcome the above limitations. Specifically, as shown in Figure 2, we propose a computation-aware Soft Pruning framework (SPViT), which simultaneously optimizes ViT accuracy and maximizes per-image dynamic pruning rate while maintaining actual computation constraints on edge devices. In ViT, each head encodes the visual receptive field independently [31, 45, 48], which implies that each token has a dif-

ferent influence in different heads [21, 25, 77, 82]. We thus propose a token selector to evaluate the importance score of each token based on its characteristic statistics in all heads. Then, through an attention-based branch [32] in the selector, we calculate the weighted sum of each score to obtain the final score of a token, which determines whether the token should be pruned. With the token selector, all tokens generated from the input images can be precisely ranked and pruned based on their importance scores and thus achieving a high overall pruning rate.

The token representations [4, 10, 65, 68] in early and middle layers are insufficiently encoded, which makes token pruning quite difficult. To mitigate the challenge, we introduce a package token technique, which compresses the less-informative tokens, picked out by the token selector, into a package token. Then, we concatenate the package token to the remaining tokens for subsequent blocks. On the one hand, although informative tokens may be discarded due to the poor encoding ability in earlier blocks of ViT [70], this error will be partly corrected by the residual information stored in the package token. On the other hand, background features can help emphasize foreground features [73]. Completely removing less informative (negative) tokens will weaken self-attention’s ability to capture key information. Therefore, the package token can serve as a way to help preserve background features. By adding minimal computation cost, the token pruning rate will be increased significantly.

In addition, we elaborate a computation-aware training strategy, which consists of two parts: computation-aware loss function and layer-to-phase progressive training. The former bridges the token pruning rates with computation resources of diverse edge devices. The latter indicates that we progressively insert one selector in each block and train the new selector under the budget constraints of the target device. Next, we group adjacent blocks with similar pruning rates into a phase, keep the first selector in this phase and remove others. While maintaining high accuracy, it can

search for the appropriate pruning rate for each block and the desired insertion position of the selector.

Our contributions are summarized as follows:

- We provide a detailed analysis on the computational complexity of ViT and different compression strategies. Based on our analysis, token pruning holds a greater computation reduction compared to the compression of other dimensions.
- Considering the vision pattern inside ViT, we propose SPViT, which includes the attention-based multi-head token selector and the token packaging technique to achieve per-image adaptive pruning. We design a computation-aware training strategy, which efficiently explores the SPViT design space given the hardware resource budget, and maximizes the per-image pruning rate without any accuracy degradation.
- SPViT enables a higher pruning rate than other state-of-the-art with comparable accuracy. For lightweight models, SPViT allows the DeiT-S and DeiT-T to reduce inference latency by 40%-60% within 0.5% accuracy loss. It can further generate more efficient and accurate PiTs compared with the model scaling [60] of original models. In particular, SPViT is superior in compression of lightweight models.
- We demonstrate a real-time realization of DeiT-T on mobile phones (e.g., 26 *ms* on a Samsung Galaxy S20) and DeiT-S on a Xilinx FPGA (13.2 *ms* on a Xilinx ZCU102). To the best of our knowledge, it is the first time that the ViT models perform inference on the edge devices beyond real-time.¹

2. Related Work

Vision Transformers. ViT [21] is a pioneering work that uses only a Transformer to solve various vision tasks. Compared to traditional CNN structures, ViT allows all the positions in an image to interact through transformer blocks, whereas CNNs operate on a fixed-sized window with restricted spatial interactions, which can have trouble capturing relations at the pixel level in both spatial and time domains [52]. Since then, many variants have been proposed [2, 9, 23, 26, 29, 41, 43, 58, 63, 64, 67, 78]. For example, DeiT [60], T2T-ViT [80] and Mixer [13] tackle the data-inefficiency problem in ViT by training only with ImageNet. PiT [31] replaces the uniform structure of Transformer with depth-wise convolution pooling layer to reduce spacial dimension and increase channel dimension. LV-ViT [35] introduces a token labeling approach to improve training. PS-ViT [81] abandons the fixed length tokens with progressive sampled tokens.

Efficient ViT. The huge memory usage and computation cost of the self-attention mechanism serve as the road-

block to the efficient deployment of the ViT model on edge devices. Many works aim at accelerating the inference speed of ViT [5]. For instance, S²ViTE [11] prunes token and attention head in a structured way via sparse training. VTP [86] reduces the input feature dimension by learning their associated importance scores with L1 regularization. IA-RED² [48] drops redundant tokens with a multi-head interpreter. PS-ViT (T2T) [59] discards useless patches in a top-down paradigm. DynamicViT [53] removes redundant tokens by estimating their importance score with a MLP [61] based prediction module. Evo-ViT [70] develops a slow-fast token evolution method to preserve more image information during pruning. TokenLearner [55] uses spatial attention to generate a small set of token vectors adaptive to the input. However, to the best of our knowledge, our idea of considering actual edge device deployment and acceleration has not been investigated by any existing ViT pruning approaches.

3. Computational Complexity Analysis

Given an input sequence $N \times D$, where N is the input sequence length or the token number and D is the embedding dimension [60] of each token, some works [48, 86] address the computational complexity of ViT as $(12ND^2 + 2N^2D)$. However, D represents different dimensions and should be written as $(4ND_{ch}D_{attn} + 2N^2D_{attn} + 8ND_{ch}D_{fc})$. Neglecting the difference may cause misleading conclusions, especially when analyzing the validity of pruning methods such as token pruning and dimension pruning.

Table 1 shows an analysis of each operation in a Transformer block. There are three main branches of ViT pruning. (i) Token channel pruning: The sequence tokens are pruned along D_{ch} dimension. D_{ch} is non-transmissible, which means reducing input dimension only affects the computation of the current matrix multiplication. To reduce computation for all layers, a mask layer is added to multiply with the input before going through the linear layer [86]. (ii) Token pruning: N is transitive, so directly pruning tokens will contribute to the linearly or even quadratically (N^2 in ② and ③) reduction of all operations. (iii) Attention head pruning (or attention channel pruning): The pruning operations are performed on weight tensors of each attention head in the MSA module. However, only the D_{attn} in the MSA module can be counted towards computation reduction, which usually contributes less than 40% of the total computation in most ViT architectures. Therefore, with the same pruning rate, pruning tokens (reducing N) can reduce more overall computation than pruning channels (reducing D_{ch} or D_{attn}).

¹Real-time inference usually means 30 frames per second, which is approximately 33 *ms* / image.

#	Module	Input Size	Operation	Layer Size	Output Size	Computation
①	MSA	$N \times D_{ch}$	Linear Transformation	$D_{ch} \times D_{attn}$	$N \times D_{attn}$	$ND_{ch}D_{attn} \times 3$
②		$N \times D_{attn}$	Q Multiplying K^T	-	$N \times N$	N^2D_{attn}
③		$N \times N$	Multiplying V	-	$N \times D_{attn}$	N^2D_{attn}
④		$N \times D_{attn}$	Projection	$D_{attn} \times D_{ch}$	$N \times D_{ch}$	$ND_{attn}D_{ch}$
⑤	FNN	$N \times D_{ch}$	FC Layer	$D_{ch} \times 4D_{fc}$	$N \times 4D_{fc}$	$4ND_{ch}D_{fc}$
⑥		$N \times 4D_{fc}$	FC Layer	$4D_{fc} \times D_{ch}$	$N \times D_{ch}$	$4ND_{fc}D_{ch}$
Total Computational Complexity						$4ND_{ch}D_{attn} + 2N^2D_{attn} + 8ND_{ch}D_{fc}$

Table 1. The computational complexity of each operation in a ViT block. The input $N \times D_{ch}$ goes through three linear transformation layers with $D_{ch} \times D_{attn}$ to generate Query (Q), Key (K), and Value (V) matrices of size $N \times D_{attn}$. N is transitive, while D_{ch} is not.

4. Computation-Aware Soft Pruning

In this section, we first introduce our soft token pruning framework. Then, we show an elaborate design of each module. Finally, we give a detailed discussion of our computation-aware training strategy.

4.1. Framework Overview

Our soft pruning framework includes a token selector and a token packaging technique. We propose a hierarchical pruning scheme, where these two modules are inserted between multiple blocks throughout the model. As shown in Figure 2, the input token sequence first goes through a token selector, where each token is scored and defined as either informative or less informative. After that, less informative tokens are separated from the sequence and integrated into a package token. This package token then concatenates to the informative tokens to involve in subsequent calculations in the blocks. In the next phase, a newly generated package token will connect with the existing package token.

For ViT training with our framework, we devise a computation-aware sparsity loss for the hardware’s maximum computation bandwidth. We perform a layer-to-phase progressive training schedule to compress the search space, where model accuracy optimization and hardware computation reduction can be simultaneously achieved. The overall framework is hardware friendly with no unsupported operations and miniature computation cost.

4.2. Attention-based Multi-head Token Selector

Multi-head Token Selector. We propose a fine-grained approach to evaluate token scores. As shown in Figure 3, in ViT’s multi-head vision pattern, each head focus on encoding different features and respective fields of an image. This implies that the importance of each token towards each head is different. Our multi-head selector generates a list of token scores for each head. Let one head dimension be $d=C/H$, where C is the input dimension and H is the number of head. We split the input $X \in \mathbb{R}^{N \times C}$ by the number of attention head into

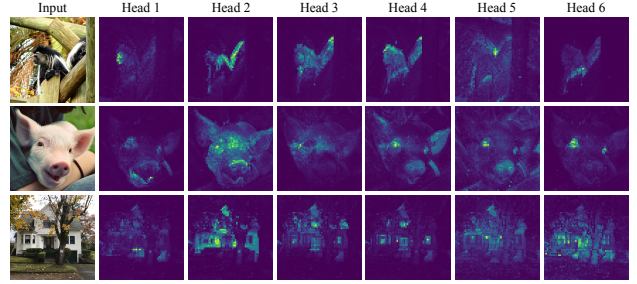


Figure 3. Heatmaps showing the informative region detected by each head in DeiT-S. Each attention head focuses on encoding different image features and visual receptive fields.

$\{x_i\}_{i=1}^H \in \mathbb{R}^{N \times d}$, and obtain local f_i^{local} and global f_i^{global} features separately through an MLP layer with a pipeline of $LayerNorm \rightarrow Linear(d, d/2) \rightarrow GELU$:

$$f_i^{local} = \text{MLP}(x_i) \in \mathbb{R}^{N \times d/2}, \quad (1)$$

$$f_i^{global} = \text{AvgPool}(\text{MLP}(x_i), D) \in \mathbb{R}^{1 \times d/2}, \quad (2)$$

where D is the keep/prune decision of the current tokens evaluated by Eq. (7). We then pass the combined feature $f_i = [f_i^{local}, f_i^{global}] \in \mathbb{R}^{N \times d}$ through a MLP pipeline of $Linear(d, d/2) \rightarrow GELU \rightarrow Linear(d/2, d/4) \rightarrow GELU \rightarrow Linear(d/4, 2)$ to produce a series of token score maps $\{t_i\}_{i=1}^H \in \mathbb{R}^{N \times 2}$, with t_i indicating the token score from each attention head:

$$t_i = \text{Softmax}(\text{MLP}(f_i)) \in \mathbb{R}^{N \times 2}, \quad (3)$$

where $N \times 2$ represents the keep and prune probabilities of N number of tokens.

Head Attention Branch. We merge the individual score maps by the weights of each attention head to get the overall token score. As shown in Figure 2, we add an attention-based branch along the selector backbone to synthesis the importance of each head:

$$\bar{X} = \text{AvgPool}(X) = \text{Concat}\{\frac{1}{C} \sum_{i=1}^C x_i\}_{j=1}^H \in \mathbb{R}^{N \times H}, \quad (4)$$

$$A = \text{Sigmoid}(\text{Linear}(\text{GeLU}(\text{Linear}(\bar{X})))) \in \mathbb{R}^{N \times H}, \quad (5)$$

where \bar{X} is a head-wise statistic generated by shrinking X through its channel dimension C with global average pooling. In Eq. (5), the attention head score vector A is obtained by feeding \bar{X} into the $\text{Linear}(H, H/2) \rightarrow \text{GeLU} \rightarrow \text{Linear}(H/2, H) \rightarrow \text{Sigmoid}$ pipeline to fully capture head-wise dependencies. The overall token score is calculated by adding the token scores from each individual attention head, multiplying by their individual head score $\{a_i\}_{i=1}^H \in \mathbb{R}^{N \times 1}$:

$$\tilde{T} = \frac{\sum_{i=1}^H t_i * a_i}{\sum_{i=1}^H a_i} \in \mathbb{R}^{N \times 2}, \quad (6)$$

where \tilde{T} is the final token probability score. To make the token removing differentiable, we apply the Gumbel-Softmax technique to generate the token keep/prune decision during training:

$$D = \text{GumbelSoftmax}(\tilde{T}) \in \{0, 1\}^N. \quad (7)$$

Next, D passes on to the following layers until reaching the next token selector, where it will be updated by applying Hadamard product with the new token keep decision $D \odot D'$ during our hierarchical pruning scheme.

4.3. Token Packaging Technique

As discussed before, ViT is less accurate for evaluating token values in earlier blocks. Poor scoring may cause important tokens to be removed. Moreover, completely removing background (negative) tokens will weaken self-attention's ability to capture key information [73]. Instead of completely discarding tokens that are considered less informative, we apply a token packaging technique that integrates them into a package token. Assume there are Q less informative tokens $\hat{X} = \{n_i\}_{i=1}^Q \in \mathbb{R}^{Q \times C}$, along with their token scores $\hat{T} = \{m_i\}_{i=1}^Q \in \mathbb{R}^{Q \times 2}$. These tokens are combined into one token by:

$$P = \frac{\sum_{i=1}^Q n_i * m_i}{\sum_{i=1}^Q m_i} \in \mathbb{R}^{1 \times C}, \quad (8)$$

where P is the package token; m_i is an individual token; n_i is its corresponding score. Token P will participate in the subsequent calculations along with the informative tokens, enabling the model to correct scoring mistakes. Our overall framework is efficient, with miniature computation cost (less than 1% of the total model GFLOPs). All the operations (MLP, Softmax, Pooling, Sigmoid, etc.) are well supported on edge platforms.

4.4. Computation-Aware Training Strategy

Our computation-aware training strategy includes two parts: (1) the training objective where we introduce the

computation-aware sparsity loss to obtain the pruning rate of token constrained by the computation resources of the target devices; (2) the layer-to-phase progressive training schedule by which we can determine the location of inserted selectors and their suitable pruning rates.

Computation-Aware Sparsity Loss. In order to bridge the inference of ViT model produced by SPViT to the actual computation bound of hardware operation, we introduce a computation-aware sparsity loss \mathcal{L}_{ratio} :

$$\text{Block} = 12N'C^2 + 2N'^2C, \quad \text{Selector} = \frac{5}{8}N'C^2 + \frac{1}{2}N'C, \quad (9)$$

$$\sum_{i=1}^L (\text{Block}_i(\rho_i \cdot N) + I_i \cdot \text{Selector}_i(\rho_i \cdot N)) \leq \text{HardwareLimit}, \quad (10)$$

$$\mathcal{L}_{ratio} = \sum_{i=1}^L (1 - \rho_i - \frac{1}{B} \sum_{b=1}^B \sum_{j=1}^N D_j^{i,b})^2, \quad (11)$$

where Eq. (9) shows the computation cost of a single ViT block (see Sec. 3) and a single selector, respectively. N' is the token number in the current block, and C is the token dimension; Eq. (10) guarantees that the computation of the model should be under the limit of target edge devices after token pruning. *HardwareLimit* is the computation constraints of the target device, which can be estimated based on the hardware resources. With i being the block index, I_i is a binary variable indicating whether a selector is inserted in Block_i . ρ_i is the corresponding pruning rate such that $N' = \rho_i \cdot N$ is the number of remaining tokens. Through Eq. (9) and (10), we derive appropriate ρ_i and feed it to the final sparsity loss (11), where B is the training batch size, and $D_j^{i,*}$ (as in Eq. (7)) is token keep decision. In order to achieve per-image adaptive compression, we set the average token pruning rate of all images in one batch as the convergence target of the Eq. (11).

Training Objective. It includes the standard cross-entropy loss, soft distillation loss, and computation-aware sparsity loss. The former two are the same as the loss strategy used in DeiT [60].

$$\mathcal{L} = \mathcal{L}_{cls} + \lambda_{KL} \mathcal{L}_{KL} + \lambda_{distill} \mathcal{L}_{distill} + \lambda_{ratio} \mathcal{L}_{ratio}, \quad (12)$$

where we set $\lambda_{KL}=0.5$, $\lambda_{distill}=0.5$, $\lambda_{ratio}=2$ in all our experiments.

Layer-to-Phase Progressive Training Schedule. Based on [85], we assume that the final CLS token is strongly correlated with classification. And we use centered kernel alignment (CKA) similarity [37] to calculate the similarity of the token features in each block and the final CLS token. As shown in Figure 4, the final CLS token feature is quite different from token features in earlier blocks. It shows that the representations in earlier blocks are encoded inadequately, which proves the difficulty of pruning tokens in the earlier blocks. Combined with this encoding pattern,

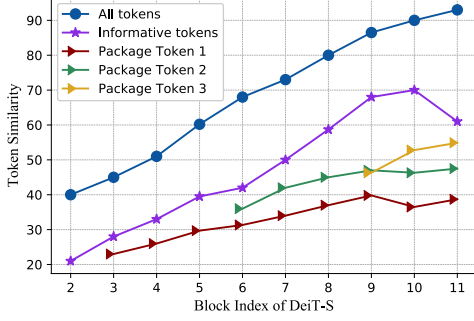


Figure 4. The CKA between the final CLS token and other tokens.

we design a computation-aware progressive training strategy to find the optimal accuracy-pruning rate trade-offs and proper locations for token selectors. In a ViT, tokens can be more effectively encoded in later blocks. Hence, we adopt progressive training on the token selector from later blocks to earlier ones. Specifically, each time we insert a token selector, we train the current selector and finetune the other parts (backbone and other selectors) by increasing the pruning rate of the current block until accuracy decreases noticeably. We repeat the insertion until there is one selector for each block. Then if the adjacent selectors have a similar pruning rate, we combine them as one selection phase and solely keep the first selector of the phase. Finally, if the final computations are lower than the computation limit of target edge devices, we reduce the pruning rate of the first selector. This is because we observe that earlier blocks are more sensitive to pruning.

5. Experiments

Datasets and Implementation Details. Our experiments are conducted on ImageNet-1K [18] with different backbones including DeiT-T, DeiT-S [60]; LV-ViT-S, LV-ViT-M [35]; PiT-T, PiT-XS, PiT-S [31]. The image resolution is 224×224 . We follow most of the training settings as in DeiT and train all backbone models for 60 epochs. Through our layer-to-phase training, we observe that inserting three token pruning selectors is best for the computation-accuracy tradeoff. For DeiT-T/S, we insert the token selector after the 3rd, 6th, and 9th layers. For LV-ViT-S, we insert the token selector after the 4th, 8th, and 12th layers. For LV-ViT-M, we insert the token selector after the 5th, 10th, and 15th layers. For PiT-T/XS/S, we insert the token selector after the 1st, 5th, and 10th layers. Our batch size is 256 for DeiT-T, DeiT-S, and LV-ViT-S; and 128 for LV-ViT-M, PiT-T, PiT-XS, and PiT-S. We set an initial learning rate to be $5e-4$ for the soft pruning module and $5e-6$ for the backbone. The final model has three token selectors. All models are trained on 8 NVIDIA A100-SXM4-40GB GPUs. The latency is measured on a Samsung Galaxy S20 cell phone that has Snapdragon 865 processor, which consists of an

Model	Method	GFLOPs	Top1 Acc (%)
PiT-S	Base Model	2.90	80.90
PiT-S	SPViT (Ours)	2.58	80.90
PiT-XS	Base Model	1.40	78.10
PiT-S	SPViT (Ours)	1.42	79.01
PiT-T	Base Model	0.71	73.00
PiT-XS	SPViT (Ours)	0.72	74.06

Table 2. Detail analysis on Pooling-based ViT with SPViT.

Octa-core Kryo 585 CPU.

5.1. Experimental Results

Main Results. We compare our method with several representative methods including DynamicViT [53], IA-RED² [48], RegNetY [51], CrossViT [6], VTP [86], ATS [24], CvT [66], PVT [64], T2T-ViT [79], UP-DeiT [76], PS-ViT [59], Evo-ViT [70], TNT [29], HVT [49], Swin [43], CoaT [69], CPVT [16], MD-DeiT [34], and S²ViTE [11]. As shown in Table 14, we report the top-1 accuracy and GFLOPs for each model. Note that “*” refers to the results reproduced with similar GFLOPs for comparison. Our SPViT reduces the computation cost by 31%~43% for various backbones with negligible 0.1%~0.5% accuracy degradation, which outperforms existing pruning methods on both accuracy and efficiency. On lightweight ViT, DeiT-T, the proposed SPViT still reduces GFLOPs by 31% with a negligible 0.1% decrease of accuracy (72.10% vs. 72.20%). To explore model scaling on ViT, we train more DeiT models with the embedding dimension of 160/256/288/320 as our baselines. On DeiT-T and DeiT-S under the same or similar GFLOPs, the accuracy improvement of SPViT over DeiT-160 is 4% (72.1% vs. 68.1% with ~ 0.9 GFLOPs), 4.67% (76.87% vs. 72.20% with ~ 1.3 GFLOPs) of SPViT-256 over DeiT-T-192, 4.82% (77.02% vs. 72.20% with ~ 1.3 GFLOPs) of SPViT-320 over DeiT-T-192, and 0.81% (79.34% vs. 78.53% with ~ 2.65 GFLOPs) of SPViT over DeiT-S-288. Additionally, our method can prune up to 23.1% on DeiT-T and 16.1% on DeiT-S without any accuracy degradation. Figure 5 demonstrates that our models achieve better accuracy-computation trade-offs compared to other pruned or scaled models.

Integrated Extension of Pooling-based ViT (PiT Series) and SPViT. Thanks to the pooling-layer mechanism, PiT filters less informative tokens the same as the downsampling process in CNN, which improves the encoding efficiency of data features. Integrated with SPViT, more efficient and accurate models can be generated. PiT-S can further reduce the computation cost by 11% without sacrificing accuracy. We compare SPViT with the embedding dimension scaling on PiT as Table 2. When compressing PiT-S to the comparable size of PiT-XS, the accuracy of the

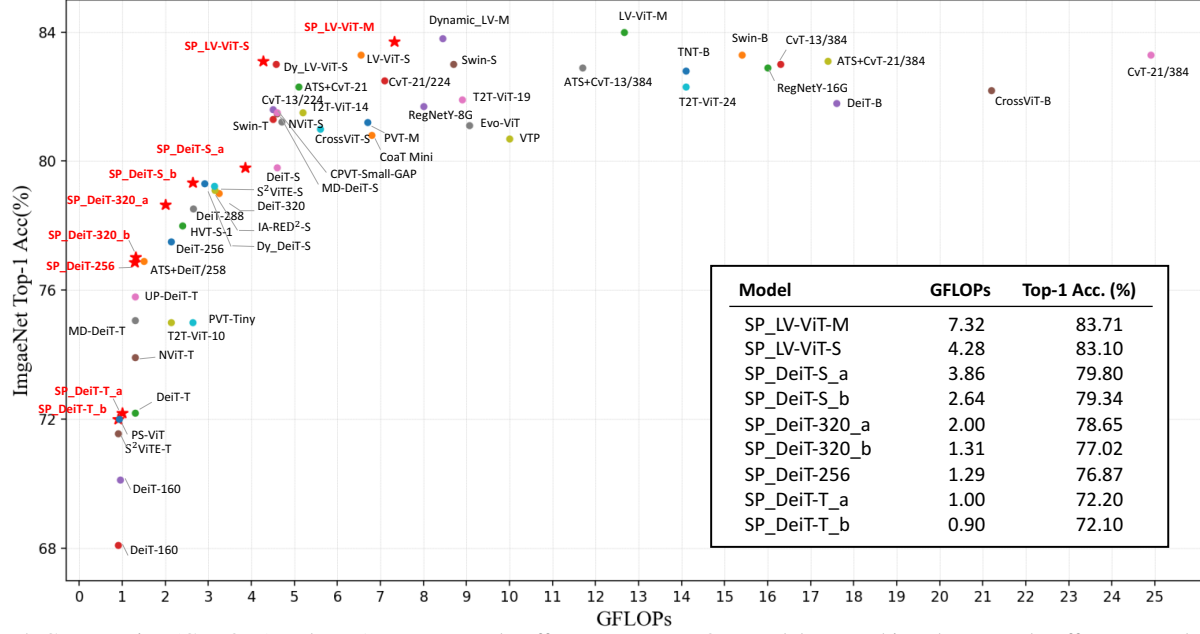


Figure 5. Computation (GFLOPs) and top-1 accuracy trade-offs on ImageNet. Our models can achieve better trade-offs compared to other pruned or scaled models.

produced model is 0.91% higher than the original PiT-XS; When the target size is PiT-T, the accuracy of the produced model is 0.9% higher than the original PiT-T.

5.2. Deployment on Edge Devices

To evaluate the hardware performance, we implement a framework that runs the ViT model on edge devices. The evaluation is conducted on a Samsung Galaxy S20 cell phone that has a Snapdragon 865 processor, which consists of an Octa-core Kryo 585 CPU carrying high performance with good power efficiency. We use all eight cores on mobile CPUs. We report the average latency of over 100 inferences. As shown in Table 3, our method outperforms existing pruning methods on both latency and accuracy. The deficiencies of other methods mainly lie in three categories: limited pruning capability (low pruning rate) [48], non-optimal pruning dimension (number of heads) [11], and less efficient operators (e.g., Argsort.) [53]. Figure 1 shows a comparison of different models with various accuracy-latency trade-off. On the one hand, our models can outperform lightweight models such as DeiT-T by up to 4.8% under similar latency. On the other hand, we are able to reduce the latency of larger models such as DeiT-S by up to 47% (60ms vs. 113ms) with only 0.46% decrease of accuracy. Especially, SP_DeiT-T achieves 26 ms per inference on mobile CPUs, which meets the real-time requirement. As far as we know, this is the first demonstration of ViT inference over 30 fps on edge devices.

Additionally, SPViT is evaluated on an embedded FPGA platform, namely, Xilinx ZCU102. To maintain the

Model	Method	Top-1 Acc. (%)	Latency (ms)
DeiT-T	Baseline	72.20	44
	S ² ViTE	70.12	35
	DynamicViT	71.85	37
	SPViT (Ours)	72.10	26
	Baseline	79.80	113
DeiT-S	S ² ViTE	79.22	78
	IA-RED ²	79.10	80
	DynamicViT	79.30	72
	SPViT (Ours)	79.34	60

Table 3. Evaluation results on Samsung Galaxy S20 with a Snapdragon 865 processor.

Model	Method	Top-1 Acc. (%)	Latency (ms)
DeiT-T	Baseline	72.20	8.81
	SPViT (Ours)	72.10	5.60
DeiT-S	Baseline	79.80	22.31
	SPViT (Ours)	79.34	13.23

Table 4. Evaluation results on Xilinx ZCU102 FPGA board.

model accuracy on hardware, 16-bit fixed-point precision is adopted to represent all the model parameters and activation data. The comparison results with baseline models are shown in Table 4. In addition to the total latency, the average latency of the multi-head attention and MLP modules in each model is listed. Compared with the baseline, DeiT-T and DeiT-S, our method could achieve $1.57\times$ and $1.69\times$ acceleration in the total latency, respectively.

5.3. Ablation Analysis

Sub-Method Effectiveness. To evaluate the effectiveness of each sub-method, we use a single head token selector

Method	GFLOPs	Top-1 Acc. (%)	Latency (ms)
DeiT-S	4.60	79.80	113
Pruning Baseline	2.63	79.03	60
+ Multi-head	2.63	79.15	60
+ Package Token	2.64	79.28	60
+ Attention-based Branch	2.64	79.34	60

Table 5. Sub-method effectiveness evaluation on DeiT-S.

Token Selector Location	Params (M)	GFLOPs	Top-1 Acc. (%)
3-6-9	22.13	2.65	79.34
1-6-9	22.13	2.70	76.10
3-6-11	22.13	2.72	78.76
6-9	22.10	2.71	78.53
3-5-7-9	22.16	2.66	79.34

Table 6. Token selector number/location evaluation on DeiT-S.

as our pruning baseline for DeiT-S, then add up each sub-method step by step and maintain the target pruning rate consistent. The sub-methods include:

- Apply the multi-head mechanism to get multiple token scores for each attention head, then get the final token score by average pooling.
- Add the token package technique to draw information from the less informative tokens into a package token.
- Add the attention-based branch to derive the head importance score for the final token score by weighted pooling.

From Table 5, we can observe that the multi-head token selector has a 0.12% accuracy improvement compared to a single head. This proves the importance of evaluating token scores based on the encoding information of each head. After adding the token packaging technique, the accuracy is improved by 0.13%. This manifests our argument that ViT’s encoding limitations may cause informative tokens pruned, while the package token creates a remedy opportunity. Through the attention-based branch, the model is further advanced by 0.06%. This indicates that in the process of data encoding, it is also different for the impact of each head. Meanwhile, each technique will introduce a small computation cost, but the latency of the hardware inference remains unchanged.

Token Selector Number and Location. After progressive training (each selector is fine-tuned by 25 epochs), we can get the pruning rate of each block as shown in Figure 6. Based on the trend of the figure, we can divide the evolution of the pruning rate into 2 phases, 3 phases, and 4 phases. We keep the appropriate selectors accordingly and re-finetuning the whole model. In Table 6, the 3-6-9 division style has the highest accuracy and the lowest computation cost, just like 3-5-7-9. According to the test on Samsung Galaxy S20, each selector and corresponding package token will introduce a delay of 1.67 ms, so that we choose 3-6-9 as the best. For another 3-phase style, 1-6-9, the accuracy and computation cost are both not ideal. This shows that due to insufficient encoding, it is difficult to perform token pruning in the earlier blocks of ViTs. Meanwhile, for the 3-6-11

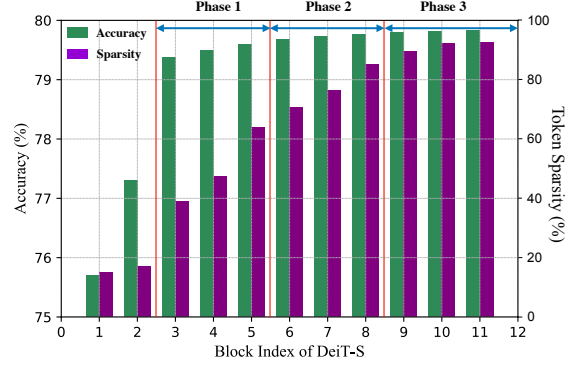


Figure 6. The accuracy and the token sparsity distribution after the Layer-to-Phase Progressive Training. We do the insertion behind the $Block_{index}$. Our final phase plan is demonstrated above.

Method	Params (M)	GFLOPs	Top-1 Acc. (%)
Baseline	22.10	4.60	79.80
1 × Package Token	22.13	2.63	79.26
+ Attention-based Branch	22.13	2.64	79.30
3 × Package Token	22.13	2.64	79.28
+ Attention-based Branch	22.13	2.64	79.34

Table 7. Package token number comparison on DeiT-S

style, both the accuracy and computation cost are slightly inferior to the 3-6-9 style. The possible reason is the pruning rate of the second phase should be smaller than the third phase and the coverage of the second phase is too wide. As a result, there is still a lot of redundancy in the tokens of the third phase, restricting the accuracy and computation efficiency of the model at the same time. Furthermore, because of a similar reason, the 2-phase style, 3-6, cannot achieve a better trade-off between accuracy and the computation cost.

Number of Package Tokens. We insert three soft pruning modules for hierarchical pruning for all models. In each module, a new package token is generated. We conduct two ways to pass on the package token for subsequent layers: 1) Merge the package token generated from the current module with the existing one from the last module by element-wise addition. Therefore, only 1 additional token is added to the input sequence in total. 2) Concatenate the new package token to the existing ones. Making it 3 additional tokens in total. Table 7 shows a comparison of the two methods.

6. Conclusion

In this paper, we propose a dynamic, computation-aware soft token pruning framework called SPViT. Our attention-based multi-head token selector and token packaging technique, along with the computation-aware training strategy can well balance the tradeoff between accuracy and specific hardware constraints. We deploy our model on mobile and FPGA, which both meet the real-time requirement.

References

- [1] Arash Amini, Arul Selvam Periyasamy, and Sven Behnke. T6d-direct: Transformers for multi-object 6d pose direct regression. *arXiv preprint arXiv:2109.10948*, 2021. [1](#)
- [2] Hangbo Bao, Li Dong, and Furu Wei. Beit: Bert pre-training of image transformers. *arXiv preprint arXiv:2106.08254*, 2021. [3](#)
- [3] Nicolas Carion, Francisco Massa, Gabriel Synnaeve, Nicolas Usunier, Alexander Kirillov, and Sergey Zagoruyko. End-to-end object detection with transformers. In *European Conference on Computer Vision (ECCV)*, pages 213–229. Springer, 2020. [1](#)
- [4] Hila Chefer, Shir Gur, and Lior Wolf. Transformer interpretability beyond attention visualization. In *Proceedings of the IEEE/CVF Conference on Computer Vision and Pattern Recognition (CVPR)*, pages 782–791, 2021. [2](#)
- [5] Boyu Chen, Peixia Li, Baopu Li, Chuming Li, Lei Bai, Chen Lin, Ming Sun, Junjie Yan, and Wanli Ouyang. Psvit: Better vision transformer via token pooling and attention sharing. *arXiv preprint arXiv:2108.03428*, 2021. [3](#)
- [6] Chun-Fu Chen, Quanfu Fan, and Rameswar Panda. Crossvit: Cross-attention multi-scale vision transformer for image classification. *arXiv preprint arXiv:2103.14899*, 2021. [1](#), [6](#), [14](#)
- [7] Haoyu Chen, Hao Tang, Nicu Sebe, and Guoying Zhao. Aniformer: Data-driven 3d animation with transformer. In *BMVC*, 2021. [1](#)
- [8] Hanting Chen, Yunhe Wang, Tianyu Guo, Chang Xu, Yiping Deng, Zhenhua Liu, Siwei Ma, Chunjing Xu, Chao Xu, and Wen Gao. Pre-trained image processing transformer. In *Proceedings of the IEEE/CVF Conference on Computer Vision and Pattern Recognition (CVPR)*, pages 12299–12310, 2021. [1](#)
- [9] Minghao Chen, Houwen Peng, Jianlong Fu, and Haibin Ling. Autoformer: Searching transformers for visual recognition. In *Proceedings of the IEEE/CVF International Conference on Computer Vision (ICCV)*, pages 12270–12280, 2021. [3](#)
- [10] Pengguang Chen, Yixin Chen, Shu Liu, Mingchang Yang, and Jiaya Jia. Exploring and improving mobile level vision transformers. *arXiv preprint arXiv:2108.13015*, 2021. [2](#)
- [11] Tianlong Chen, Yu Cheng, Zhe Gan, Lu Yuan, Lei Zhang, and Zhangyang Wang. Chasing sparsity in vision transformers: An end-to-end exploration. In *Advances in Neural Information Processing Systems*, 2021. [2](#), [3](#), [6](#), [7](#), [14](#)
- [12] Ting Chen, Saurabh Saxena, Lala Li, David J Fleet, and Geoffrey Hinton. Pix2seq: A language modeling framework for object detection. *arXiv preprint arXiv:2109.10852*, 2021. [1](#)
- [13] Xiangning Chen, Cho-Jui Hsieh, and Boqing Gong. When vision transformers outperform resnets without pre-training or strong data augmentations. *arXiv preprint arXiv:2106.01548*, 2021. [3](#)
- [14] Xin Chen, Bin Yan, Jiawen Zhu, Dong Wang, Xiaoyun Yang, and Huchuan Lu. Transformer tracking. In *Proceedings of the IEEE/CVF Conference on Computer Vision and Pattern Recognition (CVPR)*, pages 8126–8135, 2021. [1](#)
- [15] Bowen Cheng, Alexander G Schwing, and Alexander Kirillov. Per-pixel classification is not all you need for semantic segmentation. *arXiv preprint arXiv:2107.06278*, 2021. [1](#)
- [16] Xiangxiang Chu, Zhi Tian, Bo Zhang, Xinlong Wang, Xiaolin Wei, Huaxia Xia, and Chunhua Shen. Conditional positional encodings for vision transformers. *arXiv preprint arXiv:2102.10882*, 2021. [6](#), [14](#)
- [17] Zhigang Dai, Bolun Cai, Yugeng Lin, and Junying Chen. Up-detr: Unsupervised pre-training for object detection with transformers. In *Proceedings of the IEEE/CVF Conference on Computer Vision and Pattern Recognition (CVPR)*, pages 1601–1610, 2021. [1](#)
- [18] Jia Deng, Wei Dong, Richard Socher, Li-Jia Li, Kai Li, and Li Fei-Fei. Imagenet: A large-scale hierarchical image database. In *Proceedings of the IEEE/CVF Conference on Computer Vision and Pattern Recognition (CVPR)*, pages 248–255. Ieee, 2009. [6](#)
- [19] Jiajun Deng, Zhengyuan Yang, Tianlang Chen, Wengang Zhou, and Houqiang Li. Transvg: End-to-end visual grounding with transformers. *arXiv preprint arXiv:2104.08541*, 2021. [1](#)
- [20] Lei Ding, Dong Lin, Shaofu Lin, Jing Zhang, Xiaojie Cui, Yuebin Wang, Hao Tang, and Lorenzo Bruzzone. Looking outside the window: Wide-context transformer for the semantic segmentation of high-resolution remote sensing images. *arXiv preprint arXiv:2106.15754*, 2021. [1](#)
- [21] Alexey Dosovitskiy, Lucas Beyer, Alexander Kolesnikov, Dirk Weissenborn, Xiaohua Zhai, Thomas Unterthiner, Mostafa Dehghani, Matthias Minderer, Georg Heigold, Sylvain Gelly, Jakob Uszkoreit, and Neil Houlsby. An image is worth 16x16 words: Transformers for image recognition at scale. In *International Conference on Learning Representations (ICLR)*, 2021. [1](#), [2](#), [3](#)
- [22] Alaaeldin El-Nouby, Natalia Neverova, Ivan Laptev, and Hervé Jégou. Training vision transformers for image retrieval. *arXiv preprint arXiv:2102.05644*, 2021. [1](#)
- [23] Alaaeldin El-Nouby, Hugo Touvron, Mathilde Caron, Piotr Bojanowski, Matthijs Douze, Armand Joulin, Ivan Laptev, Natalia Neverova, Gabriel Synnaeve, Jakob Verbeek, et al. Xcit: Cross-covariance image transformers. *arXiv preprint arXiv:2106.09681*, 2021. [3](#)
- [24] Mohsen Fayyaz, Soroush Abbasi Kouhpayegani, Farnoush Rezaei Jafari, Eric Sommerlade, Hamid Reza Vaezi Joze, Hamed Pirsiavash, and Juergen Gall. Ats: Adaptive token sampling for efficient vision transformers. *arXiv preprint arXiv:2111.15667*, 2021. [6](#), [14](#)
- [25] Peng Gao, Jiasen Lu, Hongsheng Li, Roozbeh Mottaghi, and Aniruddha Kembhavi. Container: Context aggregation network. *arXiv preprint arXiv:2106.01401*, 2021. [2](#)
- [26] Benjamin Graham, Alaaeldin El-Nouby, Hugo Touvron, Pierre Stock, Armand Joulin, Herve Jegou, and Matthijs Douze. Levit: A vision transformer in convnet’s clothing for faster inference. In *Proceedings of the IEEE/CVF International Conference on Computer Vision (ICCV)*, pages 12259–12269, October 2021. [3](#), [13](#)
- [27] Cong Guo, Bo Yang Hsueh, Jingwen Leng, Yuxian Qiu, Yue Guan, Zehuan Wang, Xiaoying Jia, Xipeng Li, Minyi Guo,

- and Yuhao Zhu. Accelerating sparse dnn models without hardware-support via tile-wise sparsity. In *SC20: International Conference for High Performance Computing, Networking, Storage and Analysis*, pages 1–15. IEEE, 2020. 2
- [28] Meng-Hao Guo, Jun-Xiong Cai, Zheng-Ning Liu, Tai-Jiang Mu, Ralph R. Martin, and Shi-Min Hu. Pct: Point cloud transformer. *Computational Visual Media*, 7(2):187–199, Apr 2021. 1
- [29] Kai Han, An Xiao, Enhua Wu, Jianyuan Guo, Chunjing Xu, and Yunhe Wang. Transformer in transformer. In *Advances in Neural Information Processing Systems*, 2021. 3, 6, 14
- [30] Song Han, Jeff Pool, John Tran, and William J. Dally. Learning both weights and connections for efficient neural networks. In *Advances in Neural Information Processing Systems*, 2015. 2
- [31] Byeongho Heo, Sangdoo Yun, Dongyoon Han, Sanghyuk Chun, Junsuk Choe, and Seong Joon Oh. Rethinking spatial dimensions of vision transformers. In *Proceedings of the IEEE/CVF International Conference on Computer Vision (ICCV)*, 2021. 2, 3, 6
- [32] Jie Hu, Li Shen, and Gang Sun. Squeeze-and-excitation networks. In *Proceedings of the IEEE/CVF Conference on Computer Vision and Pattern Recognition (CVPR)*, pages 7132–7141, 2018. 2
- [33] Drew A Hudson and C. Lawrence Zitnick. Generative adversarial transformers. *International Conference on Machine Learning (ICML)*, 2021. 1
- [34] Ding Jia, Kai Han, Yunhe Wang, Yehui Tang, Jianyuan Guo, Chao Zhang, and Dacheng Tao. Efficient vision transformers via fine-grained manifold distillation. *arXiv preprint arXiv:2107.01378*, 2021. 6, 14
- [35] Zihang Jiang, Qibin Hou, Li Yuan, Daquan Zhou, Yujun Shi, Xiaojie Jin, Anran Wang, and Jiashi Feng. All tokens matter: Token labeling for training better vision transformers. *arXiv preprint arXiv:2104.10858*, 2021. 3, 6
- [36] Bumsu Kim, Junhyun Lee, Jaewoo Kang, Eun-Sol Kim, and Hyunwoo J Kim. Hotr: End-to-end human-object interaction detection with transformers. In *Proceedings of the IEEE/CVF Conference on Computer Vision and Pattern Recognition (CVPR)*, pages 74–83, 2021. 1
- [37] Simon Kornblith, Mohammad Norouzi, Honglak Lee, and Geoffrey Hinton. Similarity of neural network representations revisited. In *International Conference on Machine Learning (ICML)*, pages 3519–3529. PMLR, 2019. 5
- [38] Bingbing Li, Zhenglun Kong, Tianyun Zhang, Ji Li, Zhenggang Li, Hang Liu, and Caiwen Ding. Efficient transformer-based large scale language representations using hardware-friendly block structured pruning. In *Findings of the Association for Computational Linguistics: EMNLP 2020*, 2020. 2
- [39] Wenhao Li, Hong Liu, Hao Tang, Pichao Wang, and Luc Van Gool. Mhformer: Multi-hypothesis transformer for 3d human pose estimation. *arXiv preprint arXiv:2111.12707*, 2021. 1
- [40] Zhaoshuo Li, Xingtong Liu, Nathan Drenkow, Andy Ding, Francis X Creighton, Russell H Taylor, and Mathias Unberath. Revisiting stereo depth estimation from a sequence-to-sequence perspective with transformers. In *Proceedings of the IEEE/CVF International Conference on Computer Vision (ICCV)*, pages 6197–6206, 2021. 1
- [41] Yahui Liu, Enver Sangineto, Wei Bi, Nicu Sebe, Bruno Lepri, and Marco De Nadai. Efficient training of visual transformers with small-size datasets. *arXiv preprint arXiv:2106.03746*, 2021. 3
- [42] Zhuang Liu, Jianguo Li, Zhiqiang Shen, Gao Huang, Shoumeng Yan, and Changshui Zhang. Learning efficient convolutional networks through network slimming. In *Proceedings of the IEEE/CVF International Conference on Computer Vision (ICCV)*, pages 2736–2744, 2017. 2
- [43] Ze Liu, Yutong Lin, Yue Cao, Han Hu, Yixuan Wei, Zheng Zhang, Stephen Lin, and Baining Guo. Swin transformer: Hierarchical vision transformer using shifted windows. *International Conference on Computer Vision (ICCV)*, 2021. 3, 6, 14
- [44] Zhisheng Lu, Hong Liu, Juncheng Li, and Linlin Zhang. Efficient transformer for single image super-resolution. *arXiv preprint arXiv:2108.11084*, 2021. 1
- [45] Mingyuan Mao, Renrui Zhang, Honghui Zheng, Peng Gao, Teli Ma, Yan Peng, Errui Ding, and Shumin Han. Dual-stream network for visual recognition. In *Advances in Neural Information Processing Systems*, 2021. 2
- [46] Tim Meinhardt, Alexander Kirillov, Laura Leal-Taixe, and Christoph Feichtenhofer. Trackformer: Multi-object tracking with transformers. *arXiv preprint arXiv:2101.02702*, 2021. 1
- [47] Ishan Misra, Rohit Girdhar, and Armand Joulin. An End-to-End Transformer Model for 3D Object Detection. In *Proceedings of the IEEE/CVF International Conference on Computer Vision (ICCV)*, 2021. 1
- [48] Bowen Pan, Yifan Jiang, Rameswar Panda, Zhangyang Wang, Rogerio Feris, and Aude Oliva. Ia-red²: Interpretability-aware redundancy reduction for vision transformers. In *Advances in Neural Information Processing Systems*, 2021. 2, 3, 6, 7, 14
- [49] Zizheng Pan, Bohan Zhuang, Jing Liu, Haoyu He, and Jianfei Cai. Scalable vision transformers with hierarchical pooling. In *Proceedings of the IEEE/CVF International Conference on Computer Vision (ICCV)*, pages 377–386, 2021. 6, 14
- [50] Sebastian Prillo and Julian Eisenschlos. Softsort: A continuous relaxation for the argsort operator. In *International Conference on Machine Learning (ICML)*, pages 7793–7802. PMLR, 2020. 2
- [51] Ilija Radosavovic, Raj Prateek Kosaraju, Ross Girshick, Kaiming He, and Piotr Dollár. Designing network design spaces. In *Proceedings of the IEEE/CVF Conference on Computer Vision and Pattern Recognition (CVPR)*, pages 10428–10436, 2020. 6, 14
- [52] Maithra Raghu, Thomas Unterthiner, Simon Kornblith, Chiyuan Zhang, and Alexey Dosovitskiy. Do vision transformers see like convolutional neural networks? *arXiv preprint arXiv:2108.08810*, 2021. 3
- [53] Yongming Rao, Wenliang Zhao, Benlin Liu, Jiwen Lu, Jie Zhou, and Cho-Jui Hsieh. Dynamicvit: Efficient vision transformers with dynamic token sparsification. In *Advances*

- in *Neural Information Processing Systems*, 2021. 2, 3, 6, 7, 14
- [54] Ao Ren, Tianyun Zhang, Shaokai Ye, Jiayu Li, Wenyao Xu, Xuehai Qian, Xue Lin, and Yanzhi Wang. Admm-nn: An algorithm-hardware co-design framework of dnns using alternating direction methods of multipliers. In *Proceedings of the Twenty-Fourth International Conference on Architectural Support for Programming Languages and Operating Systems*, pages 925–938, 2019. 2
- [55] Michael S. Ryoo, AJ Piergiovanni, Anurag Arnab, Mostafa Dehghani, and Anelia Angelova. Tokenlearner: What can 8 learned tokens do for images and videos? In *Advances in Neural Information Processing Systems*, 2021. 3
- [56] Victor Sanh, Thomas Wolf, and Alexander M Rush. Movement pruning: Adaptive sparsity by fine-tuning. *arXiv preprint arXiv:2005.07683*, 2020. 2
- [57] Aravind Srinivas, Tsung-Yi Lin, Niki Parmar, Jonathon Shlens, Pieter Abbeel, and Ashish Vaswani. Bottleneck transformers for visual recognition. In *Proceedings of the IEEE/CVF Conference on Computer Vision and Pattern Recognition (CVPR)*, pages 16519–16529, 2021. 1
- [58] Andreas Steiner, Alexander Kolesnikov, Xiaohua Zhai, Ross Wightman, Jakob Uszkoreit, and Lucas Beyer. How to train your vit? data, augmentation, and regularization in vision transformers. *arXiv preprint arXiv:2106.10270*, 2021. 3
- [59] Yehui Tang, Kai Han, Yunhe Wang, Chang Xu, Jianyuan Guo, Chao Xu, and Dacheng Tao. Patch slimming for efficient vision transformers, 2021. 3, 6, 14
- [60] Hugo Touvron, Matthieu Cord, Matthijs Douze, Francisco Massa, Alexandre Sablayrolles, and Hervé Jégou. Training data-efficient image transformers & distillation through attention. In *International Conference on Machine Learning (ICML)*, 2021. 1, 3, 5, 6
- [61] Ashish Vaswani, Noam Shazeer, Niki Parmar, Jakob Uszkoreit, Llion Jones, Aidan N Gomez, Łukasz Kaiser, and Illia Polosukhin. Attention is all you need. In *Advances in neural information processing systems*, pages 5998–6008, 2017. 1, 3
- [62] Hanrui Wang, Zhekai Zhang, and Song Han. Spatten: Efficient sparse attention architecture with cascade token and head pruning. In *2021 IEEE International Symposium on High-Performance Computer Architecture (HPCA)*, pages 97–110. IEEE, 2021. 2
- [63] Pichao Wang, Xue Wang, Fan Wang, Ming Lin, Shuning Chang, Wen Xie, Hao Li, and Rong Jin. Kvt: k-nn attention for boosting vision transformers. *arXiv preprint arXiv:2106.00515*, 2021. 3
- [64] Wenhai Wang, Enze Xie, Xiang Li, Deng-Ping Fan, Kaitao Song, Ding Liang, Tong Lu, Ping Luo, and Ling Shao. Pyramid vision transformer: A versatile backbone for dense prediction without convolutions. In *Proceedings of the IEEE/CVF International Conference on Computer Vision (ICCV)*, 2021. 3, 6, 14
- [65] Bichen Wu, Chenfeng Xu, Xiaoliang Dai, Alvin Wan, Peizhao Zhang, Zhicheng Yan, Masayoshi Tomizuka, Joseph Gonzalez, Kurt Keutzer, and Peter Vajda. Visual transformers: Token-based image representation and processing for computer vision. *arXiv preprint arXiv:2006.03677*, 2020. 2
- [66] Haiping Wu, Bin Xiao, Noel Codella, Mengchen Liu, Xiyang Dai, Lu Yuan, and Lei Zhang. Cvt: Introducing convolutions to vision transformers. *arXiv preprint arXiv:2103.15808*, 2021. 6, 14
- [67] Kan Wu, Houwen Peng, Minghao Chen, Jianlong Fu, and Hongyang Chao. Rethinking and improving relative position encoding for vision transformer. In *Proceedings of the IEEE/CVF International Conference on Computer Vision (ICCV)*, pages 10033–10041, 2021. 3
- [68] Chenfeng Xu, Bohan Zhai, Bichen Wu, Tian Li, Wei Zhan, Peter Vajda, Kurt Keutzer, and Masayoshi Tomizuka. You only group once: Efficient point-cloud processing with token representation and relation inference module. *arXiv preprint arXiv:2103.09975*, 2021. 2
- [69] Weijian Xu, Yifan Xu, Tyler Chang, and Zhuowen Tu. Co-scale conv-attentional image transformers. *arXiv preprint arXiv:2104.06399*, 2021. 6, 14
- [70] Yifan Xu, Zhijie Zhang, Mengdan Zhang, Kekai Sheng, Ke Li, Weiming Dong, Liqing Zhang, Changsheng Xu, and Xing Sun. Evo-vit: Slow-fast token evolution for dynamic vision transformer. *arXiv preprint arXiv:2108.01390*, 2021. 2, 3, 6, 14
- [71] Fanglei Xue, Qiangchang Wang, and Guodong Guo. Transfer: Learning relation-aware facial expression representations with transformers. In *Proceedings of the IEEE/CVF International Conference on Computer Vision (ICCV)*, pages 3601–3610, 2021. 1
- [72] Bin Yan, Houwen Peng, Jianlong Fu, Dong Wang, and Huchuan Lu. Learning spatio-temporal transformer for visual tracking. *arXiv preprint arXiv:2103.17154*, 2021. 1
- [73] Ceyuan Yang, Zhirong Wu, Bolei Zhou, and Stephen Lin. Instance localization for self-supervised detection pretraining. In *Proceedings of the IEEE/CVF Conference on Computer Vision and Pattern Recognition (CVPR)*, pages 3987–3996, 2021. 2, 5
- [74] Fuzhi Yang, Huan Yang, Jianlong Fu, Hongtao Lu, and Bain-ing Guo. Learning texture transformer network for image super-resolution. In *Proceedings of the IEEE/CVF Conference on Computer Vision and Pattern Recognition (CVPR)*, pages 5791–5800, 2020. 1
- [75] Guanglei Yang, Hao Tang, Mingli Ding, Nicu Sebe, and Elisa Ricci. Transformer-based attention networks for continuous pixel-wise prediction. In *Proceedings of the IEEE/CVF International Conference on Computer Vision (ICCV)*, 2021. 1
- [76] Hao Yu and Jianxin Wu. A unified pruning framework for vision transformers. *arXiv preprint arXiv:2111.15127*, 2021. 6, 14
- [77] Qihang Yu, Yingda Xia, Yutong Bai, Yongyi Lu, Alan Yuille, and Wei Shen. Glance-and-gaze vision transformer. In *Advances in Neural Information Processing Systems*, 2021. 2
- [78] Kun Yuan, Shaopeng Guo, Ziwei Liu, Aojun Zhou, Fengwei Yu, and Wei Wu. Incorporating convolution designs into visual transformers. In *Proceedings of the IEEE/CVF International Conference on Computer Vision (ICCV)*, pages 579–588, October 2021. 3

- [79] Li Yuan, Yunpeng Chen, Tao Wang, Weihao Yu, Yujun Shi, Zihang Jiang, Francis EH Tay, Jiashi Feng, and Shuicheng Yan. Tokens-to-token vit: Training vision transformers from scratch on imagenet. *arXiv preprint arXiv:2101.11986*, 2021. 6, 14
- [80] Li Yuan, Yunpeng Chen, Tao Wang, Weihao Yu, Yujun Shi, Zi-Hang Jiang, Francis E.H. Tay, Jiashi Feng, and Shuicheng Yan. Tokens-to-token vit: Training vision transformers from scratch on imagenet. In *Proceedings of the IEEE/CVF International Conference on Computer Vision (ICCV)*, pages 558–567, October 2021. 3
- [81] Xiaoyu Yue, Shuyang Sun, Zhanghui Kuang, Meng Wei, Philip H.S. Torr, Wayne Zhang, and Dahua Lin. Vision transformer with progressive sampling. In *Proceedings of the IEEE/CVF International Conference on Computer Vision (ICCV)*, pages 387–396, October 2021. 3
- [82] Xiaohua Zhai, Alexander Kolesnikov, Neil Houlsby, and Lucas Beyer. Scaling vision transformers. *arXiv preprint arXiv:2106.04560*, 2021. 2, 13
- [83] Hengshuang Zhao, Li Jiang, Jiaya Jia, Philip HS Torr, and Vladlen Koltun. Point transformer. In *Proceedings of the IEEE/CVF International Conference on Computer Vision (ICCV)*, pages 16259–16268, 2021. 1
- [84] Sixiao Zheng, Jiachen Lu, Hengshuang Zhao, Xiatian Zhu, Zekun Luo, Yabiao Wang, Yanwei Fu, Jianfeng Feng, Tao Xiang, Philip HS Torr, et al. Rethinking semantic segmentation from a sequence-to-sequence perspective with transformers. In *Proceedings of the IEEE/CVF Conference on Computer Vision and Pattern Recognition (CVPR)*, pages 6881–6890, 2021. 1
- [85] Daquan Zhou, Yujun Shi, Bingyi Kang, Weihao Yu, Zihang Jiang, Yuan Li, Xiaojie Jin, Qibin Hou, and Jiashi Feng. Refiner: Refining self-attention for vision transformers, 2021. 5
- [86] Mingjian Zhu, Kai Han, Yehui Tang, and Yunhe Wang. Visual transformer pruning. In *KDD 2021 Workshop on Model Mining*, 2021. 3, 6, 14

A. Analysis and Discussion

A.1. Model Scaling

In ViTs, the most common method to scale the model is to change the number of channels, while our SPViT provides another perspective to perform token pruning for better complexity/accuracy trade-offs. We illustrate this superior effect of SPViT in Figure 7. First, we train several DeiT [25] models with varying embedding dimensions from 192 to 384. Second, we compress these DeiT into ones whose channel has one less head than them. However, these new compressed models (SPViT-serious) have better accuracy than DeiT original variants with similar computation. Specifically, the orange line of SPViT-serious is closer to the upper left corner of the Figure 7 than the original DeiT-serious. For DynamicViT, we have also observed uniform benefits, but its efficient models are still slightly inferior to SPViT.

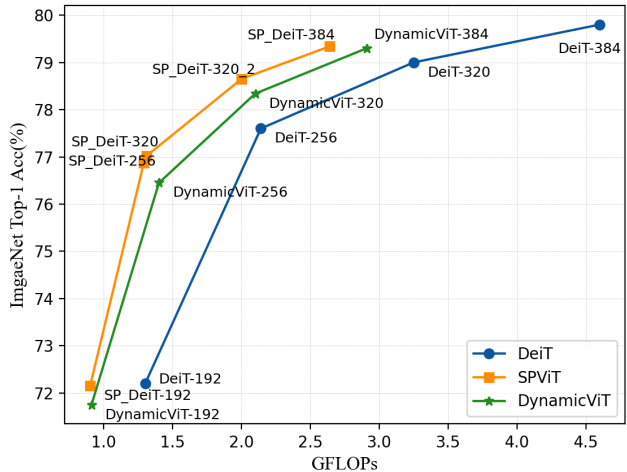


Figure 7. Comparison of our SPViT method with model scaling. We prune DeiT models with embedding dimensions varying from 192 to 384 and compare with DynamicViT under comparable GFLOPs.

A.2. Progressive Training Sparsity for Each Layer

As a supplement for Figure 6, we show the exact sparsity and accuracy of each layer for our progressive training in Table 8. We start by adding the token selector one by one from the 11th layer to the 1st layer. The layer index indicates the layer before the token selector. Between 6~8 and 9~11 layer, each layer has similar accuracy and sparsity, which indicates that these layers can be combined to one pruning phase with a token selector at the front.

A.3. Model Latency on Hardware

We show all model latency results tested on Samsung Galaxy S20 in Table 9. On the one hand, our models

Layer	1	2	3	4	5	6	7	8	9	10	11
Accuracy	75.7	77.3	79.4	79.5	79.6	79.7	79.7	79.7	79.8	79.8	79.8
Sparsity	0.15	0.17	0.39	0.47	0.64	0.71	0.77	0.85	0.89	0.92	0.93

Table 8. Progressive training sparsity for each layer

can outperform lightweight models such as DeiT-T by up to 4.8% with even smaller latency (38ms vs. 44ms). On the other hand, we are able to reduce the latency of larger models such as DeiT-S by up to 47% (60ms vs. 113ms) with only 0.46% decrease in accuracy. On LV-ViT-S/M, our SPViT models show better performance, outperforming DynamicViT on both latency and accuracy.

Model	Method	Top-1 Acc. (%)	Latency (ms)
DeiT-T	Baseline	72.20	44
	S ² ViTE	70.12	35
	DynamicViT	71.85	37
	SPViT (Ours)	72.20	33
	SPViT (Ours)	72.10	26
	SPViT-256 (Ours)	76.87	36
DeiT-S	Baseline	79.80	113
	S ² ViTE	79.22	78
	IA-RED ²	79.10	80
	DynamicViT	79.30	72
	SPViT-320 (Ours)	78.65	47
	SPViT (Ours)	79.34	60
LV-ViT-S	Baseline	83.30	148
	DynamicViT	83.00	114
	SPViT (Ours)	83.10	89
LV-ViT-M	Baseline	84.00	269
	DynamicViT	83.61	195
	SPViT (Ours)	73.71	152

Table 9. Evaluation results on Samsung Galaxy S20 with a Snapdragon 865 processor.

A.4. Comparison of Different Token Selector Designs

We analyze the performance of our token selector design by replacing it with different operations. More specifically, we replace the original MLP based pipeline in Eq. (1) and (2) with a convolution-based pipeline: $Conv1d \rightarrow BatchNorm1d \rightarrow GELU$. We also evaluated different activation functions: RELU and Hardswish. We compare these variants of the token selector on DeiT-T with a complexity of 0.9 GFLOPs. As shown in Table 10, under the same training settings, MLP based token selectors outperform convolution-based token selectors (72.10% vs 71.56%). Furthermore, GELU function outperforms Hardswish and RELU (71.56% vs. 71.48% vs. 71.13% on Conv1d+3kernel). However, we can not hastily conclude that MLP and GELU are superior to convolution and other activation functions. This may be due to different training difficulties. Hardswish is harder to converge, so larger

epochs may be necessary [26]. Additionally, Conv1d with 1 kernel can mimic MLP’s fully connected layer. The accuracy gap between these two may due to distinct desirable initial learning rates and schedulers. Result also shows that a larger kernel size may be more preferable (71.34% vs. 71.56% on Conv1d), which can help learn more local representation. We will further invest in these designs in our future work. More specifically, train each design under different training settings. Also, combining the advantages of MLP and convolution layers.

Token Selector	GFLOPs	Top-1 Acc. (%)
MLP+GELU	0.90	72.10
MLP+Hardswish	0.90	71.94
Conv1d+3kernel+RELU	0.90	71.13
Conv1d+3kernel+GELU	0.90	71.56
Conv1d+3kernel+Hardswish	0.90	71.48
Conv1d+1kernel+GELU	0.90	71.34

Table 10. Comparison of different token selector layers and activation functions

A.5. Comparison of Different Pruning Methods

To further prove the effectiveness of our score-based dynamic token pruning method, we compare with some general pruning methods: random pruning, structure pruning. For random pruning, we randomly remove the input token, neglecting the token importance. For structure pruning, we prune the input feature map by dimension, which will impair every token. Results are shown in Table 11. Under the same computational complexities (0.9 GFLOPs for DeiT-T and 2.64 GFLOPs for DeiT-S), our proposed method achieves the best accuracy.

Model	Method	GFLOPs	Top-1 Acc. (%)
DeiT-T	Random	0.90	69.87
	Structure	0.90	70.32
	Token selector	0.90	72.10
DeiT-S	Random	2.64	77.25
	Structure	2.64	77.86
	Token selector	2.64	79.34

Table 11. Comparison of different pruning method

A.6. Effectiveness of the Token Packaging Technique w/o Class Token

In many recently proposed vision transformer models, the class token was removed and replaced by doing average pooling on the last output feature to aggregate representation from all patch tokens [26, 82]. This process is similar to our token packaging technique, where we also apply average pooling on the removed tokens. We raise a

conjecture: Our token packaging technique can be more effective on models that do not rely on the class token. To test our hypothesis, we run a simple experiment by first pre-training a DeiT-T without a class token, and then applying our method both with and without the token packaging technique. As shown in Table 12, when training on a DeiT model that contains a class token, our token packaging technique can improve the performance by 0.12% (72.1% vs. 72.0%). When training on a DeiT model without a class token, our token packaging technique can improve the performance by 0.23% (70.75% vs. 70.52%), which verified our assumption.

Model	GFLOPs	Top-1 Acc. (%)
DeiT-T	1.30	72.20
SPViT	0.90	72.10
SPViT w/o package token	0.90	71.98
DeiT-T w/o cls token	1.29	71.42
SPViT	0.87	70.75
SPViT w/o package token	0.87	70.52

Table 12. Effectiveness of the token packaging technique w/o class token

A.7. Comparison of Different Batch Sizes

We run our SPViT on DeiT-S with different batch sizes for ablation. Results in Table 13 show that accuracy has a slight boost when batch size increases.

Batch Size	GFLOPs	Top-1 Acc. (%)	Top-5 Acc. (%)
96	2.65	79.31	94.64
128	2.65	79.32	94.64
256	2.64	79.34	94.67

Table 13. Different batch size comparison on DeiT-S

A.8. Encoding Redundancy of the Pooling Layer

We make further discussion on Pooling-based ViT (PiT Series). Figure 8 shows that the attention matrix before and after SPViT retains great similarity, which enlightens that the encoding redundancy of the pooling-layer mechanism can be recognized precisely by SPViT.

B. Visualization

B.1. Token Pruning Visualization

We further visualize the process of SPViT to describe the performance in the inference phase and make a comparison between the framework with the token packaging technique and without it the token packaging technique. As shown in Figure 9, row 1 and 3 show the results collected from the framework without token packaging, row 2 and 4 are

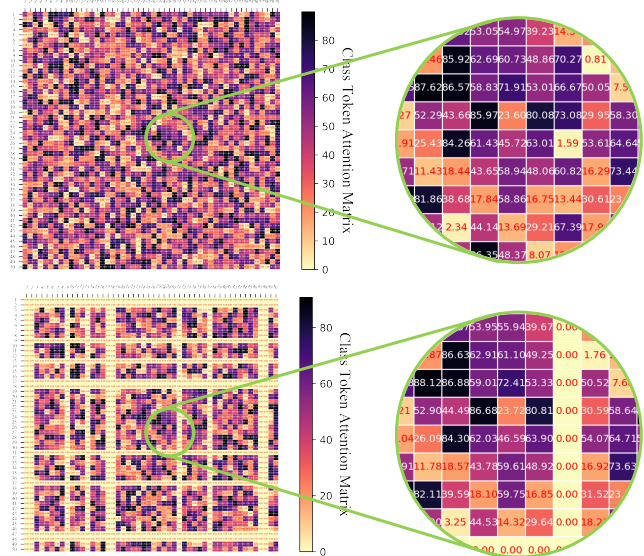


Figure 8. Illustration of the first attention matrix at the final block. Upper figure is the original PiT-S, lower one is with SPViT.

from the framework with token packaging. Take row 1 and 2 for example: At phase 1, there is a 7% difference in the left image groups and 11% in the right ones; At phase 2, 11% difference in the left image groups and 15% in the right ones; At phase 3, 14% difference in the left image groups and 18% in the right ones. We can infer token packaging can help to lock the object instead of the background. And this phenomenon is more obvious in complex and multi-object images.

B.2. Self-attention Head Heatmap

Figure 10 shows the heatmaps of informative region detected by each self-attention head in DeiT-S. Each attention head focuses on encoding different image features and visual receptive fields. Therefore, token importance is different for each head. This demonstrates the need for obtaining token score individually.

C. Main Results

We compare our method with several representative methods including DynamicViT [53], IA-RED² [48], Reg-NetY [51], CrossViT [6], VTP [86], ATS [24], CvT [66], PVT [64], T2T-ViT [79], UP-DeiT [76], PS-ViT [59], Evo-ViT [70], TNT [29], HVT [49], Swin [43], CoaT [69], CPVT [16], MD-DeiT [34], and S²ViTE [11]. As shown in Table 14, we report the top-1 accuracy and GFLOPs for each model. Note that “*” refers to the results reproduced with similar GFLOPs for comparison.

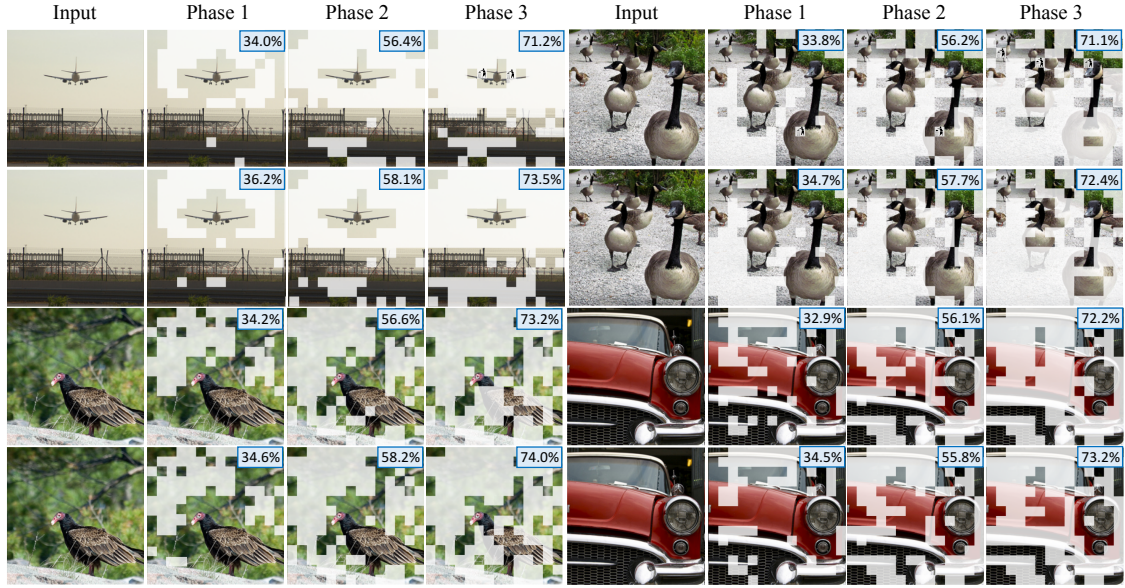


Figure 9. Visualization of each pruning phase. Row 1 and 3 show the results collected from the framework without token packaging and row 2 and 4 show the results from the framework with token packaging.

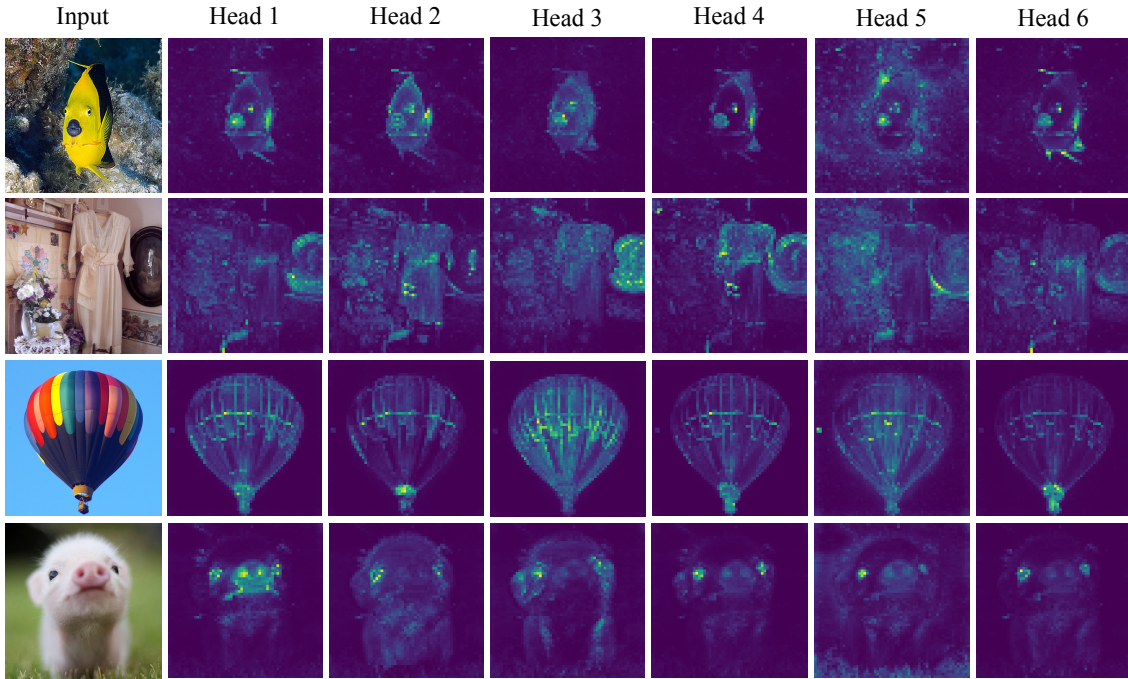


Figure 10. Heatmaps showing the informative region detected by each head in DeiT-S.

Model	Method	Params (M)	GFLOPs	GFLOPs ↓ (%)	Top-1 Acc. (%)
DeiT-T	Baseline/192	5.60	1.30	0.00	72.20
	Baseline/160*	4.00	0.90	30.77	68.10
	NViT-T	6.40	1.30	0.00	73.91
	UP-DeiT-T	5.70	1.30	0.00	75.79
	MD-DeiT-T	5.70	1.30	0.00	75.06
	T2T-ViT-10	5.90	2.13	-63.85	75.00
	PVT-Tiny	13.20	2.64	-103.08	75.00
	DynamicViT	5.90	0.91	30.00	71.85
	PS-ViT	5.60	0.93	28.46	72.00
	S ² ViTE	4.20	0.95	26.92	70.12
	ATS+DeiT/258	10.13	1.50	-15.38	76.90
	SPViT (Ours)	5.70	1.00	23.08	72.20
	SPViT (Ours)	5.70	0.90	30.77	72.10
	SPViT-256 (Ours)	10.16	1.29	0.77	76.87
	SPViT-320 (Ours)	15.44	1.30	0.00	77.02
DeiT-S	Baseline/384	22.10	4.60	0.00	79.80
	Baseline/320*	15.40	3.25	29.35	79.00
	Baseline/288*	12.60	2.65	42.39	78.53
	Baseline/256*	10.00	2.14	53.48	77.21
	HVT-S-1	22.10	2.40	47.82	78.00
	S ² ViTE	14.60	3.14	31.74	79.22
	IA-RED ²	-	3.15	31.52	79.10
	DynamicViT	22.80	2.91	36.74	79.30
	DynamicViT*	22.80	2.71	41.09	79.12
	SPViT-320 (Ours)	15.44	2.00	56.52	78.65
	SPViT (Ours)	22.13	3.86	16.09	79.80
	SPViT (Ours)	22.13	2.64	42.61	79.34
LV-ViT-S	Baseline/384	26.15	6.55	0.00	83.30
	Swin-T	29.00	4.50	31.29	81.30
	CvT-13/224	20.00	4.50	31.29	81.60
	MD-DeiT-S	22.10	4.60	29.77	81.48
	CPVT-Small-GAP	23.00	4.60	29.77	81.50
	NViT-S	23.00	4.70	28.24	81.22
	ATS+CvT-21	32.00	5.10	22.14	82.30
	T2T-ViT-14	22.00	5.20	20.61	81.50
	CrossViT-S	26.70	5.60	14.50	81.00
	PVT-Medium	44.20	6.70	-2.29	81.20
	CoaT Mini	10.00	6.80	-3.82	80.80
	DynamicViT	26.90	4.57	30.22	83.00
	SPViT (Ours)	26.17	4.28	34.65	83.10
LV-ViT-M	Baseline/512	55.83	12.67	0.00	84.00
	CvT-21/224	32.00	7.10	43.96	82.50
	DynamicViT*	57.10	7.35	41.99	83.61
	DynamicViT	57.10	8.45	33.31	83.80
	RegNetY-8G	39.00	8.00	36.86	81.70
	Swin-S	50.00	8.70	31.33	83.00
	T2T-ViT-19	39.20	8.90	29.76	81.90
	Evo-ViT	87.30	9.07	28.41	81.11
	VTP	48.00	10.00	21.07	80.70
	ATS+CvT-13/384	20.00	11.70	7.66	82.90
	T2T-ViT-24	64.10	14.10	-11.29	82.30
	TNT-B	66.00	14.10	-11.29	82.80
	Swin-B	88.00	15.40	-21.55	83.30
	RegNetY-16G	84.00	16.00	-26.28	82.90
	CvT-13/384	20.00	16.30	-28.65	83.00
	ATS+CvT-21/384	32.00	17.40	-37.33	83.10
	DeiT-B	86.60	17.60	-38.91	81.80
	CrossViT-B	104.70	21.20	-67.32	82.20
	CvT-21/384	32.00	24.90	-96.53	83.30
	SPViT (Ours)	55.85	7.32	42.23	83.71

Table 14. Results of different ViTs on ImageNet-1K. We compare the proposed SPViT with existing ViT pruning methods under comparable GFLOPs and the number of parameters. Note that “*” refers to our reproduced results to obtain models with similar GFLOPs for comparison. Negative values in FLOPs reduction mean FLOP increases. Baseline/160/192/288/384 indicates the embedding dimensions. SPViT-256/320 indicates pruning from DeiT scaling model of 256/320 embedding dimensions.